Research Article

Mohit Vij*, Neha Dand, Lalit Kumar, Neeraj Choudhary, Parveen Kumar, Pankaj Wadhwa*, Shahid Ud Din Wani, Faiyaz Shakeel, and Mohammad Ali

Novel microwave-based green approach for the synthesis of dual-loaded cyclodextrin nanosponges: Characterization, pharmacodynamics, and pharmacokinetics evaluation

https://doi.org/10.1515/gps-2024-0187
received August 24, 2024; accepted December 2, 2024

Abstract: Recently, microwave-based cyclodextrin nanosponges (CDNS) of domperidone (DOM) for their solubility and dissolution improvement have been studied. However, microwave-based CDNS for the dual-loading of cinnarizine (CIN) and DOM have not been documented. Therefore, this research concentrates explicitly on the concurrent loading of two drugs employing these nanocarriers, namely CIN and DOM, both categorized under Class II of the Biopharmaceutical Classification System. A green approach involving microwave synthesis was employed to fabricate these nanocarriers. Fourier transform infrared (FTIR) spectroscopy confirmed the formation of CDNS, while scanning electron microscopy scans illustrated their porous nature. X-ray diffraction studies established the crystalline structure of the nanocarriers. Differential scanning calorimetry and FTIR analyses corroborated the drugs' loading and subsequent amorphization. *In vitro* drug release studies demonstrated an enhanced solubility of the drugs, suggesting a potential improvement in their bioavailability. The *in vivo* pharmacokinetic investigation emphatically substantiated this hypothesis, revealing a 4.54- and 2.90-fold increase in the bioavailability of CIN and DOM, respectively. This enhancement was further supported by the results of the pharmacodynamic study utilizing the gastrointestinal distress/pica model, which indicated a significantly reduced consumption of kaolin. Conclusively, this study affirms the adaptability of microwave-based CDNS for the concurrent loading of multiple drugs, leading to improved solubility and bioavailability.

Keywords: bioavailability, cyclodextrin, microwave, nanocarriers, nanosponge

*** Corresponding author: Mohit Vij,** School of Pharmaceutical Sciences, Lovely Professional University, Phagwara, Punjab, 144411, India; Government Pharmacy College, Seraj, Himachal Pradesh, 175035, India, e-mail: mohitvij_5@yahoo.com
*** Corresponding author: Pankaj Wadhwa,** School of Pharmaceutical Sciences, Lovely Professional University, Phagwara, Punjab, 144411, India, e-mail: pankaj.23400@lpu.co.in
Neha Dand: Department of Pharmaceutics, Bharati Vidyapeeth's College of Pharmacy, Navi Mumbai, 400614, India
Lalit Kumar, **Neeraj Choudhary:** GNA School of Pharmacy, GNA University, Phagwara, Punjab, 144401, India
Parveen Kumar: Government Pharmacy College, Sullah, Kangra, Himachal Pradesh, 176084, India
Shahid Ud Din Wani: Division of Pharmaceutics, Department of Pharmaceutical Sciences, University of Kashmir, Srinagar, 190006, India
Faiyaz Shakeel: Department of Pharmaceutics, College of Pharmacy, King Saud University, Riyadh, 11451, Saudi Arabia
Mohammad Ali: Department of Pharmacology, Sri Adichunchanagiri College of Pharmacy, Adichunchanagiri University, B.G. Nagar, Nagamagala, Bellur, Karnataka, 571418, India

1 Introduction

The simultaneous administration of two or more active substances in a single dosage form to enhance therapeutic response is termed combination drug therapy [1]. This approach is advantageous for achieving a synergistic effect improving patient compliance and reducing dosing frequency, especially in chronic conditions. Pathological complexities such as cancer, neurodegenerative disorders, pain management, and infectious diseases necessitate the use of combination drug therapy for effective treatment and management [2]. Motion sickness, nausea, and vertigo are all treated with the antihistaminic drug cinnarizine (CIN) [3,4]. As an antiemetic medication, domperidone (DOM) is frequently used to temporarily reduce nausea and vomiting [5,6]. Combining CIN and DOM is more

beneficial than using either drug alone, according to clinical research on human subjects [7]. According to the Biopharmaceutical Classification System, both CIN and DOM medicines are classified as class II pharmaceuticals, meaning they have weak solubility and good permeability [8,9]. The co-administration of combined drugs in a single formulation can be facilitated by a variety of nanocarriers, such as liposomes, niosomes, organic or inorganic nanoparticles, polymeric or lipid nanoparticles, nanotubes, microemulsions, nanoemulsions, and surfactant or polymeric micelles [10,11]. Improved bioavailability, enhanced therapeutic efficacy, protection against degradation, a controlled release profile, and site-specific delivery of the pharmaceuticals under study are provided by these nanocarriers [11–14]. Nevertheless, despite ongoing advancements and impressive outcomes, the majority of the aforementioned nanocarrier types have a number of disadvantages that limit their effectiveness in combination therapy, including low drug entrapment efficiency, poor drug-loading, limited stability, potential toxicity of the nanocarrier components, and unintended side effects [11]. Recently, researchers have looked into combining drug complexation with cyclodextrins into various nanocarrier types as a potential way to get around the disadvantages of each individual nanocarrier and then increase their efficacy by combining their individual positive effects into a single nanocarrier [11,14]. Therefore, cyclodextrin nanosponges (CDNS) for dual-loaded drug delivery of CIN and DOM were selected in this study.

While native cyclodextrins have historically been successful in enhancing the solubility and stability of poorly soluble drugs, limitations such as the ability to load only one drug at a time and limited loading capacity have prompted researchers to seek solutions [15]. The emergence of cyclodextrin-based nanosponges as a carrier system addresses these challenges, offering the capability to load multiple lipophilic or hydrophilic drugs with superior capacity compared to native cyclodextrins. CDNS, polymerized derivatives of native cyclodextrins through cross-linking, possess biodegradable and non-toxic monomers, enjoying widespread regulatory acceptance in the pharmaceutical industry [16]. Previous studies on the encapsulation of various drugs like nicosulfuron [17], quercetin [18], resveratrol [19], and fisetin [20] have proven the merit of these nanocarriers in effective drug delivery.

Despite the theoretical advantages of loading multiple drugs within the same nanocarrier, few systems have explored this aspect of CDNS, likely due to the physical characteristics of these nanocarriers. Various synthetic approaches have been discussed in the literature, and the choice of method has been linked to the physicochemical properties of nanosponges. Two distinct forms of CDNS – amorphous and crystalline – have been identified, with preparation methods influencing their nature [21,22]. Traditional methods, such as fusion and solvent evaporation, were initially employed but faced challenges related to non-uniform reactions, large solvent requirements, low yield, and, more importantly, yielding nanosponges having an amorphous nature, which would lead to reduced drug loading [23]. To address these limitations, newer and more environmentally friendly techniques, such as microwave and ultrasonic-assisted synthesis, have gained attention. These methods seek to enhance the morphological, physical, and functional properties of nanosponges. The shift to these microwave-based approaches is driven by the need for straightforward, inexpensive, quick, and scalable procedures for the mass manufacturing of monodisperse, stable nanosponges with regulated size and shape [24]. Recently, we reported microwave-based CDNS of DOM for its solubility and dissolution improvement [25]. However, microwave-based CDNS for the combined therapy of CIN and DOM has not been documented. Therefore, the present research has focused on the microwave-mediated synthesis of crystalline CDNS, demonstrating their potential in complexing with poorly soluble model drugs – CIN and DOM. The goal is to enhance these drugs' solubility, dissolution, and oral bioavailability while achieving a controlled release profile.

2 Materials and methods

2.1 Materials

CIN and DOM were graciously supplied as gift samples by Ankur Drugs and Pharma Ltd. (Baddi, India). β-Cyclodextrin (βCD) was generously provided by Roquette India Pvt., Ltd. (Mumbai, India). Diphenylcarbonate (DPC) and dimethylformamide (DMF) were procured from Sigma Aldrich (Mumbai, India). All additional chemicals and reagents utilized in this study were of analytical grade. Milli Q water (Millipore) was employed throughout the experimental procedures.

2.2 Synthesis of blank and dual drug-loaded CDNS

Using a fiber optic temperature sensor with an infrared camera and a magnetic stirring system, microwave reactions were conducted at 2,450 MHz in a scientific microwave system (Raga Tech, Bangalore, India). This integrated

system proved to be useful in upholding and monitoring the reaction conditions required for the synthesis of nanosponge materials. The process involved the mixing of 100 mL of DMF with the monomer (βCD) and cross linker (DPC) in various molar ratios in a 250 mL flask before microwave irradiation. The solvent was extracted using a distillation procedure following a predetermined amount of time spent carrying out the reaction. To purify the final product after complete solvent removal, it was first washed with water and then extracted using a Soxhlet apparatus with ethanol for 4 h. The obtained formulation was optimized to get stable and insoluble blank nanosponges, which are referred to as microwave-nanosponges (MW-NS) [23]. Equimolar proportions of the drugs and the MW-NS were equilibrated under slow-stirring, centrifuged to remove uncomplexed drugs, and finally lyophilized using a lyophilizer (Bio gene, India) to obtain dual drug-loaded MW-NS.

2.3 Physicochemical characterization of dual drug-loaded MW-NS

2.3.1 Particle size, polydispersity index (PDI), and zeta potential

The average size, PDI, and zeta potential of dual drug-loaded MW-NS were assessed with a "Malvern® Zetasizer Nano ZS 90 (Malvern® Instruments Limited, Worcestershire, UK)." Each test sample was diluted 200 times with deionized water before three measurements were taken at a fixed scattering angle of 90° and a temperature of 25°C, respectively.

2.3.2 Drug loading and entrapment efficiency

To get rid of any leftover medication, 50 mg of dual drug-loaded MW-NS was thoroughly cleaned with methanol. To release the medication contained, they were sonicated for 15 min after being dried and further triturated with methanol. After filtering, the solutions were examined using high-performance liquid chromatography (HPLC) at 270 nm and spectrophotometry at 254 and 287 nm [26]. Using standard formulae, the drug encapsulation efficiency was calculated.

2.3.3 Fourier transform infrared-attenuated total reflectance (FTIR-ATR) spectroscopy

The FTIR-3000B (Analytical Technologies Ltd., Mumbai, India) was used to produce FTIR-ATR spectra for both blank and dual drug-loaded MW-NS in the 4,000–600 cm^{-1} frequency range. To prevent contamination, each spectrum was recorded in a dry atmosphere with a sensitivity of 4 cm^{-1}. The resulting average of over 100 repeats produced a satisfactory signal-to-noise ratio and reproducibility.

2.3.4 Differential scanning calorimetry (DSC)

A Hitachi, DSC 7020 calorimeter (Tokyo, Japan) was used for the DSC analysis. The heat of fusion and indium melting point were used to calibrate the device. Heating was done at a pace of 10°C per minute to reach temperatures between 35 and 300°C. An empty sample pan was used as a reference when sourcing aluminum sample pans. Five-milligram samples were examined in triplicate while under nitrogen purge.

2.3.5 X-ray powder diffraction (XRPD)

We used a Bruker diffractometer (D8 Advance, Coventry, UK) to conduct a comprehensive XRPD investigation to investigate the differential crystallinity behavioral patterns of blank MW-NS and dual drug-loaded MW-NS. The chosen specimens were photographed over a 2θ range across a 5–90° angle at a 40 kV voltage and 40 mA current utilizing copper wire as a radiation source.

2.3.6 Morphological studies

Using field emission scanning electron microscopy (SEM) (JSM-7610F Plus, JEOL, Tokyo, Japan), the surface morphology of both blank and dual drug-loaded MW-NS was examined. The nanosponges were carelessly dispersed across a double-sided carbon adhesive tape. Then, to lessen the charging effects, those were hit on 300 Å gold-coated aluminum stubs, and photomicrographs were obtained at an accelerating voltage of 20 kV.

2.4 *In vitro* drug release and release kinetics

Using the USP dissolution tester apparatus II (Paddle type, Lab, India), release tests were conducted for plain medicines, dual drug-loaded MW-NS, and the physical mixing of the medications with βCD. At 37 ± 0.5°C, the temperature was maintained while the paddles rotated at 50 rpm. Dialysis bags were filled with amounts of pure CIN and DOM with and without βCD, as well as dual drug-loaded MW-NS equal to 20 mg of CIN and 15 mg of DOM. After being submerged in

the release medium, the dialysis bags were fastened to a paddle. After the initial release tests were carried out in 900 mL of 0.1 N HCl (pH 1.2) for 2 h, the dialysis bag sample was transferred to a hemispherical dissolution container with 900 mL of pH 6.8 phosphate buffer for a further 22 h. Five-milliliter samples were removed after 2, 4, 6, 8, 10, 12, and 24 h and replaced with an equivalent volume of the new drug-free medium. Spectrophotometric analysis was performed on the filtered samples at wavelengths of 254 and 287 nm. The average values of the three distinct release studies were displayed as the cumulative percentage of drugs released over time. Furthermore, release profiles between dual drug-loaded MW-NS and plain drug combinations were compared using the f_1 and f_2 values. Many kinetic models were used to analyze the drug release from dual drug-loaded MW-NS. The best model for determining the release mechanism was chosen [27] based on the coefficient of determination (R^2).

2.5 Pharmacokinetic studies

A single-dose, randomized block trial design was selected for this investigation. Male albino Wistar rats, around 6 weeks old and weighing 250–300 g, were used in this experiment. The Wistar rats were starved for 24 h before receiving treatment [28]. The study animals were divided into four groups, each consisting of six individuals. Group I, which was given an oral dose of the pure drug combination (CIN + DOM) suspension in distilled water, was regarded as the positive control group. Group II was regarded as a negative control group since it was given blank MW-NS in distilled water. The oral-marketed tablet containing the combination of DOM and CIN was given to the animals in Group III through oral gavage. The tablet was dissolved in distilled water and then taken orally. Group IV was given MW-NS which was dual drug-loaded. Group IV received the same dosage of DOM and CIN as a market tablet formulation plus a positive control.

Blood from each rat's retro-orbital plexus vein was continuously collected at 1, 2, 3, 8, 12, 24, 36, and 48 h intervals [29]. The time points for the blood collection were based on the time to reach the maximum plasma concentration (T_{max}) of both drugs. The T_{max} of CIN in healthy human volunteers after oral administration has been reported to be 1–3 h with a mean value of 2 h [30]. However, the average T_{max} of DOM in healthy male volunteers after oral administration has been reported to be 1.2 h [31]. The reported T_{max} values of CIN and DOM indicated that both drugs would reach their maximum plasma concentration (C_{max}) values before 3 h of administration (absorption phase) [30,31]. After reaching C_{max}, the elimination phase started. Therefore, initially, the blood sampling was carried out frequently (1, 2, and 3 h) after that it was delayed due to the start of the elimination phase (8, 12, 24, and 48 h). Heparinized containers were used to collect the blood samples, and red blood cells were whirled at 3,000 rpm for 30 min to enable them to settle. After being collected in tubes, the supernatant plasma was housed at −20°C before being assessed using the established HPLC technique [26]. The pharmacokinetic parameters following oral administration of different formulations were estimated for each rat in each group. The values of C_{max} and T_{max} were directly read from the plasma concentration–time profile curves. The values of area under curve from time 0–t (AUC_{0-48}), area under curve from time$_{0-\infty}$ ($AUC_{0-\infty}$), clearance (Cl), volume of distribution (V_d), elimination rate constant (K_{el}), mean residence times (MRT), and elimination half-life ($t_{1/2}$) for CIN and DOM were derived from the plasma concentrations of CIN and DOM vs time plot using the non-compartmental method.

2.6 Pharmacodynamics study

Male albino Wistar rats ranging between 250 and 300 g were employed in the investigation. Prior to administration, the Wistar rats were fasted for 24 h. This pharmacodynamics study was carried out by using the rat emesis model. Using a brusque oral needle as an emetic inducer, an oral dosage of 40 mg·kg^{-1} of copper sulfate in distilled water was delivered to the rats intragastrically to measure their degree of pica [32]. The gram count of kaolin ingested by rats is used to measure pica [33]. A thick paste was made by blending 1:100 w/w of hydrated kaolin and acacia gum with distilled water. Kaolin pellets were made to imitate the normal food of rats kept in the lab. The pellets were allowed to air dry at room temperature.

Pica was constantly monitored for 48 h after receiving test materials (dual drug-loaded MW-NS in 1 mL of distilled water suspension) orally 10 min before emetic stimulation. The ingestion of these kaolin pellets within the first 24 and 48 h after the drug's administration provided the pica data. To get the final number, the consumption of the dual drug-loaded MW-NS group was subtracted from the consumption of the control group.

2.7 HPLC analysis

The HPLC technique employed in the current investigation adheres to the methodology previously elucidated by Sirisha and Kumari [34]. Chromatographic isolation of the two pharmaceutical compounds was executed utilizing a C-18 column with dimensions of 250 mm × 4.6 mm i.d., and a particle size

of 5 µm. The mobile phase, comprising a mixture of acetonitrile and methanol in a volumetric ratio of 30:70 v/v, was delivered at a flow rate of 1 mL·min^{-1}. An autosampler facilitated the injection of 10 µL of the prepared solution, and the detection of the compounds was accomplished at a wavelength of 270 nm. Both the sample solutions and the mobile phase were degassed and filtered through a 0.45 µm membrane filter (Millipore, USA) before analysis.

2.8 Statistical analysis

With GraphPad Prism Software (version 9.4.1, San Diego, CA, USA), the statistical test was run. To compare the two groups, an independent *t*-test was run, and for multiple group comparisons, a *post hoc* Tukey's test was run after the one-way analysis of variance. For results with a *p*-value of below 0.05, they were deemed statistically significant.

2.9 Ethical approval

The research related to animal use has been complied with all the relevant national regulations and institutional policies for the care and use of animals. The protocol was reviewed and approved for ethical conduct by the PBRI, Bhopal's Institutional Animal Ethics Committee prior to the experiment's execution. The study's protocol number was PBRI/IAEC/29-03/010.

3 Results and discussion

3.1 Synthesis of blank and dual drug-loaded nanosponges

Initially, conventional methods, such as fusion and solvent evaporation, were used to prepare CDNS. However, these methods produced non-uniform reactions, large amounts of solvent consumption, and low yield. The yield of CDNS using fusion and solvent evaporation methods was found to be 31.58% and 40.61%, respectively. However, the yield of CDNS using a microwave-based approach was recorded to be 77.80%. Microwave-based synthesis stands out as a highly advantageous method for crafting cyclodextrin-based nanosponges due to its unique features. This technique offers unparalleled efficiency and speed, significantly reducing reaction times compared to conventional methods [35]. The ability to precisely control reaction conditions under microwave irradiation ensures reproducibility and consistency in nanosponge preparation [36]. The rapid and uniform heating provided by microwaves enhances the overall yield of the synthesis process [37]. Additionally, the simplicity and ease of operation associated with microwave synthesis contribute to its appeal [38]. The method proves particularly beneficial for cyclodextrin-based nanosponges, as it facilitates the formation of well-defined, crystalline structures with desirable properties [39]. Overall, microwave synthesis emerges as a robust and time-efficient approach, holding promise for advancing the production of these innovative nanomaterials. Thus, it was opted to use microwave irradiation as a technique to synthesize these dual drug-loaded cyclodextrin-based nanosponges.

3.2 Particle size, PDI, and zeta potential

The zeta potential value for dual drug-loaded MW-NS was found to be −8.69 ± 0.36 mV, which was deemed adequate to prevent particle collisions caused by electric repulsion. The formulation's particle size of 198.3 ± 1.7 nm confirmed its nano-size. The PDI value of 0.242 is commonly recognized as a moderately dispersed nature of nanocarriers [40].

3.3 Entrapment efficiency

The entrapment competence of dual drug-loaded MW-NS was 80.60 ± 1.56% for CIN and 79.00 ± 2.08% for DOM. Substantial encapsulation efficiencies within the formulation may plausibly stem from the incorporation of active components into the non-polar interstices inherent in the molecular arrangement of nanosponge entities. This behavior can also be explained by H-bond formation, which is made possible by the presence of H-atoms on the active species, or by interactions between aromatic rings and the protons connected to βCD that result in strong van der Waals forces [41,42]. As a result, the high entrapment efficiencies of CIN and DOM were possible due to the presence of βCD, which forms inclusion complexes with hydrophobic drugs like CIN and DOM [11]. This inclusion of complex formation could also maximize the drug-loading efficiencies for both drugs.

3.4 FTIR-ATR

FTIR-ATR was used to assess if the pharmaceutical substance could be encapsulated by the nanosponges. Figure 1 shows the FTIR spectra of the medicines, blank MW-NS, and dual drug-loaded MW-NS. Characteristic peaks for C–H stretching (aromatic, alkene, mono-substituted), C═C (aromatic stretch),

–CH_2 (alkane), and C–N stretching were shown by CIN at 2,959, 1,597, 1,490, 1,448, and 1,134 cm^{-1}, respectively [43]. At the same time, DOM showed peaks at 3,126, 2,933, 1,718, and 1,693 cm^{-1}, which were attributed to N–H bending, C═O stretching, asymmetric C–H stretching, and N–H stretching, respectively [44]. The cross-linking procedure is complete when the spectra of blank MW-NS do not show the typical non-hydrogen-bonded O–H stretching peak at 3,350 cm^{-1}, which is attributed to the primary alcohol group in βCD. Additionally, the presence of a peak around 1,750 cm^{-1} is indicative of carbonate cross-linked MW-NS. These observations have been reported by previous researchers [45–47]. During the drug loading and encapsulation phases, characteristic drug peaks were anticipated to diminish, decrease in intensity, or exhibit a shift in wave number. In the spectrum of dual drug-loaded MW-NS, all prominent peaks associated with CIN and DOM appeared at markedly low intensity [29]. Notably, the distinctive peak at around 1,780 cm^{-1} and no peak at 3,350 cm^{-1} suggest the successful formation of nanosponges and the concurrent encapsulation of both drugs in combination.

3.5 DSC

The typical βCD peaks were detected between 316°C and 328°C, while the DPC (linker) peaks were seen between 72°C and 74°C (Figure 2). The absence of these peaks in the dual drug-loaded MW-NS suggested that the reaction had occurred and that the individual components were missing. It also emphasizes how well the post-synthesis cleaning mechanism worked. The peak temperatures of the medicines CIN and DOM are 118°C and 254°C, respectively. The presence of both peaks in the dual drug-loaded MW-NS suggests that there was no chemical reaction between the medicines (Figure 3). The drug peaks have decreased, suggesting that the drug was trapped in the generated nanosponges and that these nanosponges later amorphized [29,48].

3.6 XRPD

The XRPD analysis, as depicted in Figure 4a, substantiates the crystalline nature of βCD. In contrast, the XRD pattern of CDNS synthesized through conventional methods, as illustrated in Figure 4b, exhibited diffuseness devoid of discernible peaks, indicative of the amorphous configuration of the polymer. The XRD profile of blank MW-NS, presented in Figure 4c, manifested alterations in peak intensities along with a distinct peak pattern, suggesting the crystalline or para-crystalline characteristics of the resultant nanosponge [49].

The XRPD patterns of CIN and DOM, as illustrated in Figure 5a and b, respectively, unequivocally verify their crystalline structures. The physical mixture's XRD pattern is shown in Figure 5c as a composite representation that overlays the separate patterns of βCD, CIN, and DOM. Contrarily, the diffraction pattern of the dual drug-loaded MW-

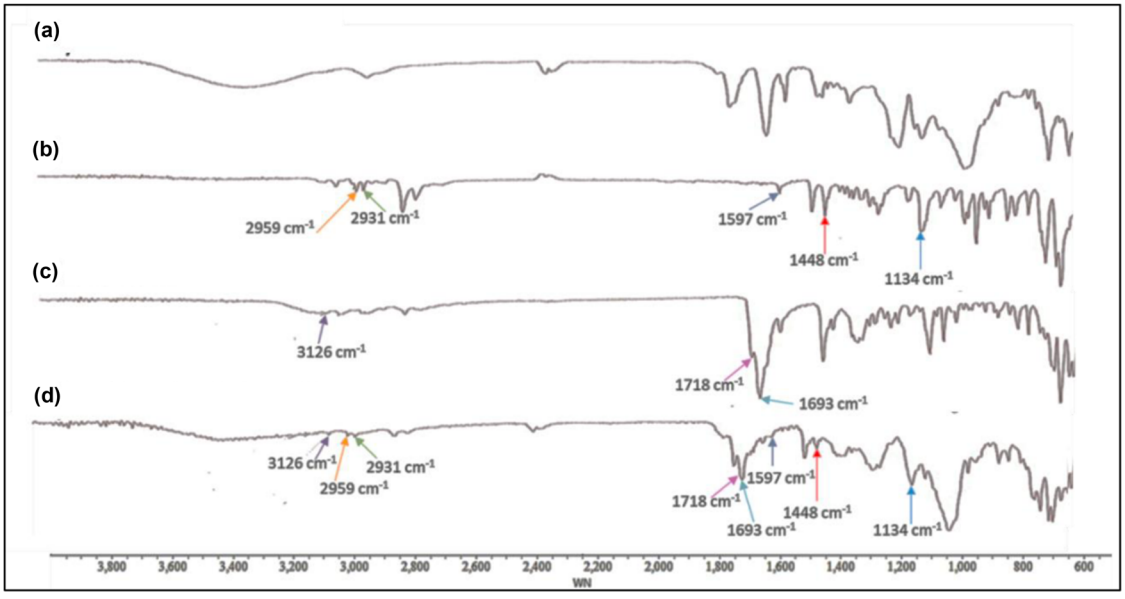

Figure 1: FTIR spectra of (a) blank MW-NS, (b) plain CIN, (c) plain DOM, and (d) dual drug-loaded MW-NS.

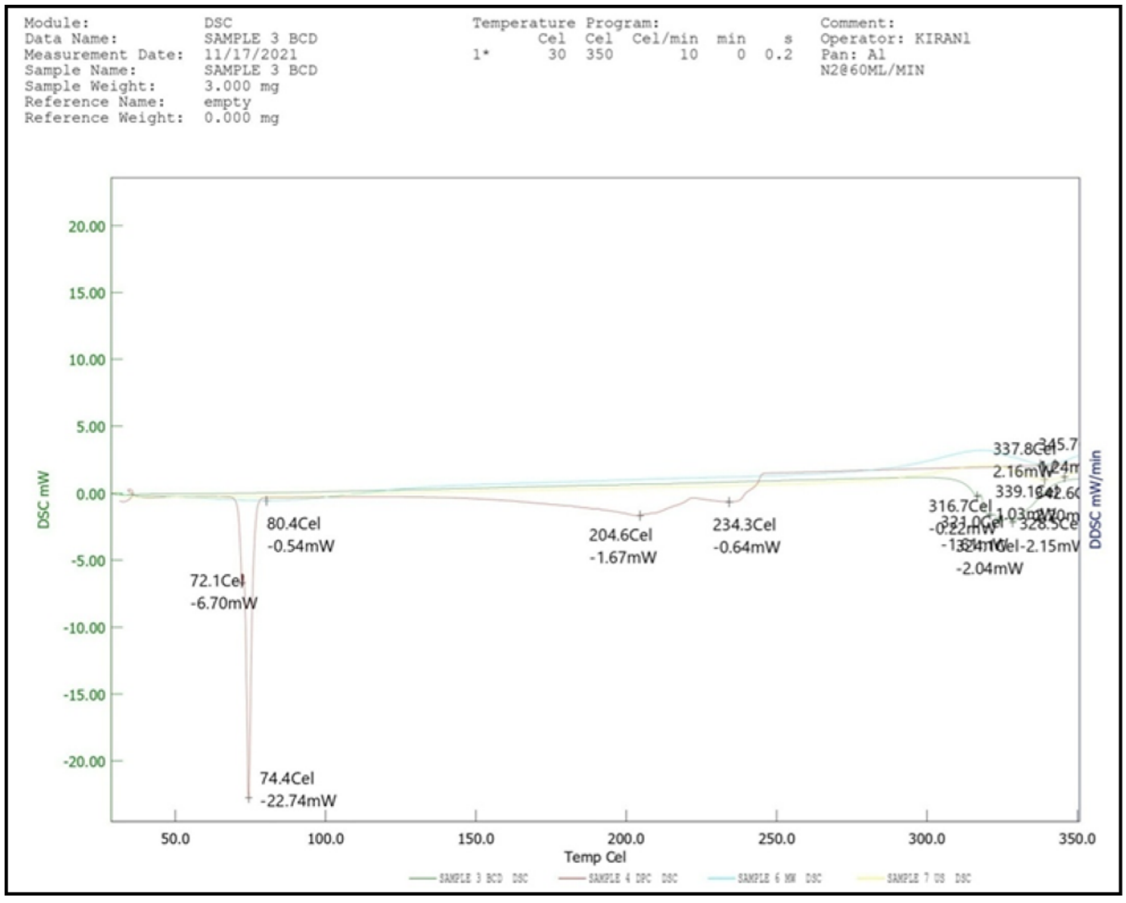

Figure 2: DSC curves of βCD, DPC, and dual drug-loaded MW-NS.

NS (Figure 5d) attests to its crystalline/para-crystalline nature, distinct from the individual patterns of CIN and DOM. This disparity implies the encapsulation of both drugs within the nanosponge, potentially resulting in their amorphization [16,50]. The amorphization of MW-NS indicated the changes in the physicochemical properties of CIN and DOM. This would result in enhanced solubility of CIN and DOM in nanosponges [11,26]. This improvement in solubility would ultimately result in improved drug release and overall bioavailability of CIN and DOM [11].

3.7 Morphological evaluation

Through experiments using SEM, the shape of the particles was assessed. Figure 6a and b displays the SEM topography pictures of βCD and dual drug-loaded MW-NS, respectively. The crystalline character of βCD is illustrated by an SEM picture. Samples with the characteristic sponge-like conformation of βCD nanosponges were seen when βCD molecules were joined together with the use of a linker to produce nanosponges. A recent study reports that following lyophilization, nanosponges maintain their distinctive sponge-like shape. Our samples' porosity might help with the enhanced loading and delivery of medications [51]. Other researchers have also reported a similar porous nature of these nanosponges as detected by SEM scanning [51,52].

3.8 *In vitro* drug release studies

Figures 7 and 8 show the drug release profiles of CIN and DOM, respectively. Table 1 lists the corresponding f_1 and f_2 values. The application of nanosponges, particularly those synthesized via microwave techniques, demonstrates a statistically significant enhancement in drug release profiles. Notably, nanosponges exhibit a remarkable 2- to 3-fold increase in the release of CIN compared to the plain drug and physical mixture counterparts, achieving a release ranging from 60% to 70% within 24 h ($p < 0.05$). Furthermore, for DOM, the nanosponge formulation results in a

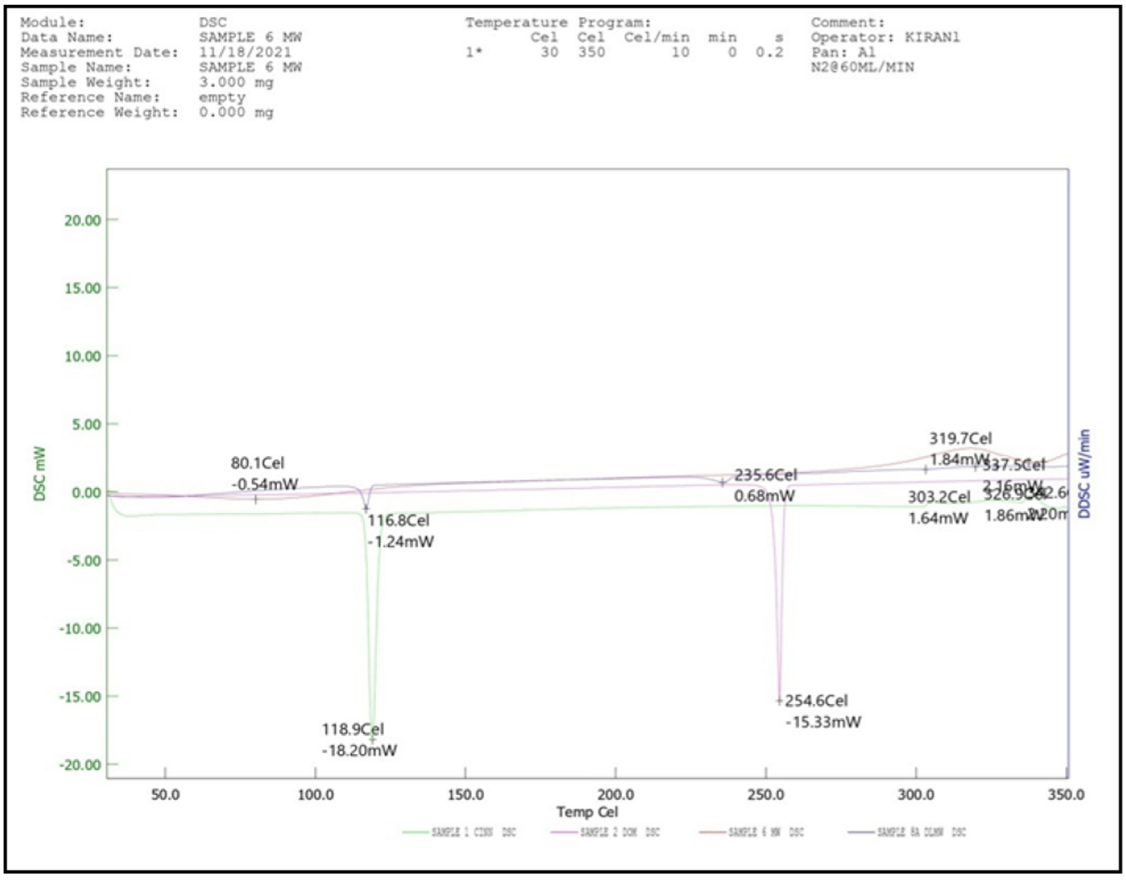

Figure 3: DSC curves of CIN, DOM, and dual drug-loaded MW-NS.

sustained release profile with a statistically significant difference in the cumulative release compared to the plain drug and physical mixture ($p < 0.01$). The initial release of DOM from nanosponges, albeit slightly lower at 30–40%, becomes highly significant as it surpasses 80% by the end of the 24-h period. The significant release profiles of CIN and DOM from nanosponges were possible due to the nanometer range particle size of dual drug-loaded nanosponges (198.3 nm) compared to plain drug and physical mixture. In addition, the improvement in the solubility and porosity of dual drug-loaded nanosponges could be the other reason for the significant release of CIN and

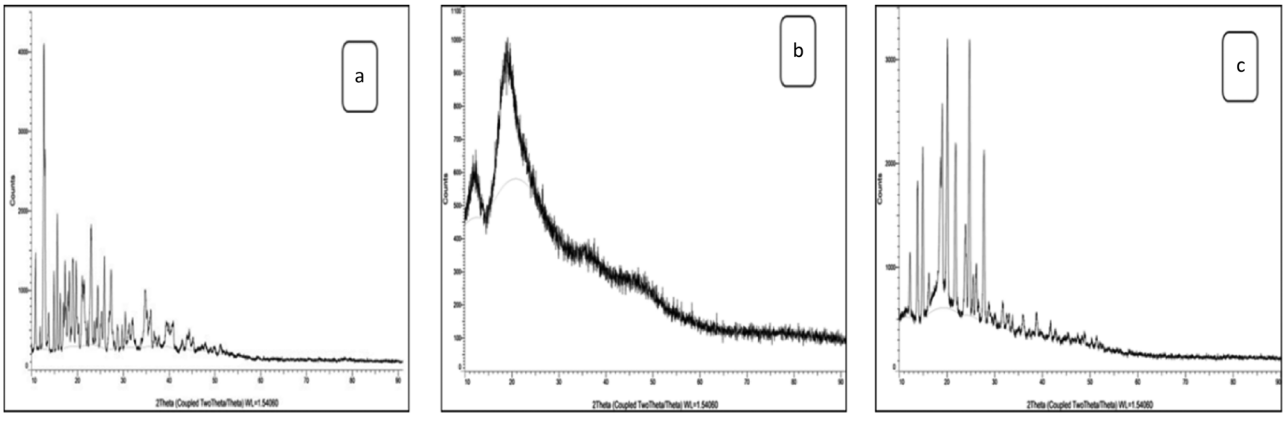

Figure 4: XRPD spectra of (a) βCD, (b) blank nanosponges prepared by the melt method, and (c) blank nanosponges prepared by the microwave-based technique.

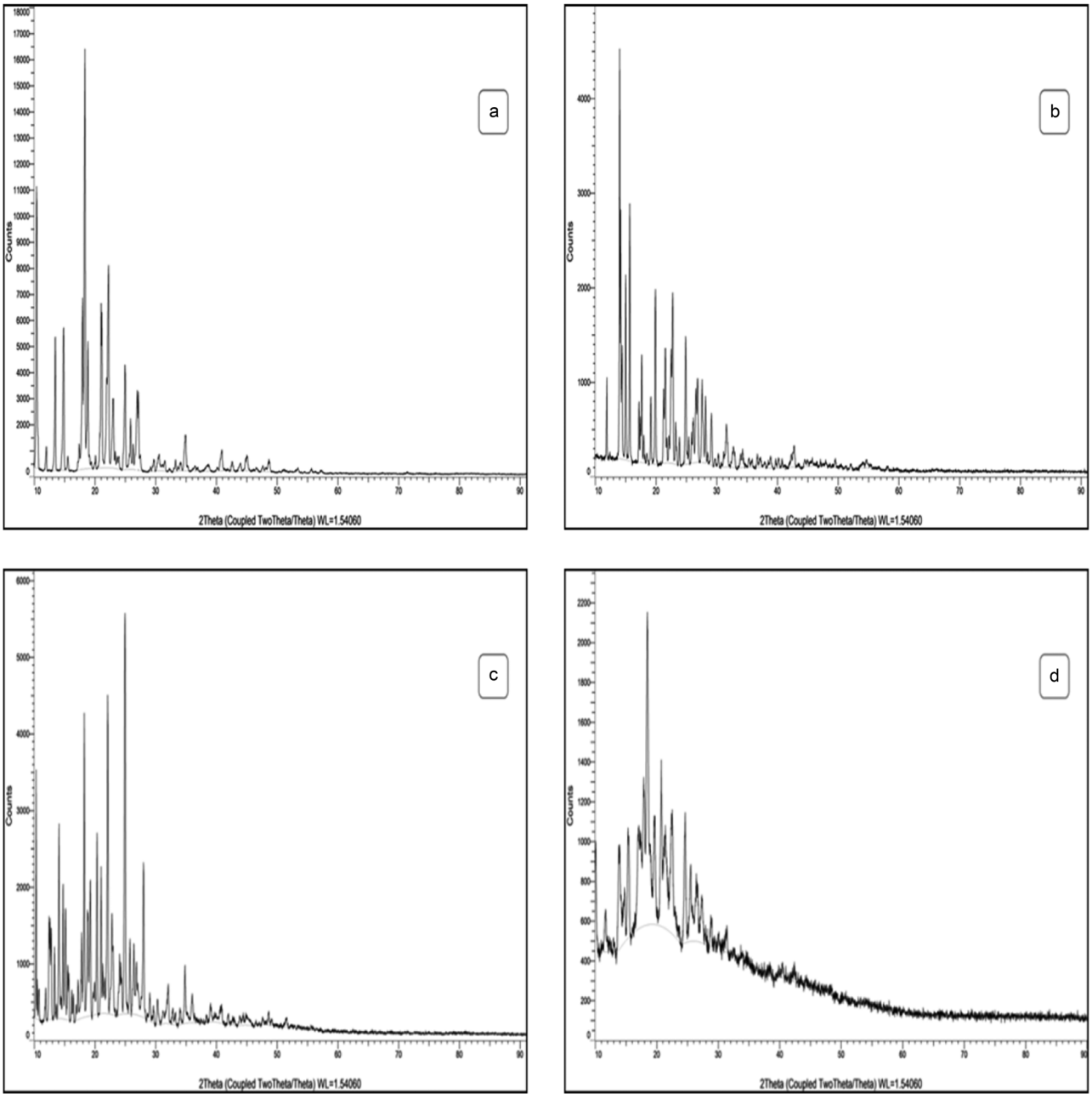

Figure 5: XPRD spectra of (a) CIN, (b) DOM, (c) physical mixture and βCD, and (d) dual drug-loaded loaded MW-NS.

DOM from nanosponges compared to the plain drugs and physical mixture. These statistically robust findings underscore the efficacy of nanosponges, especially those prepared innovatively, as a statistically significant and promising strategy for controlled and prolonged drug release, thus presenting a statistically justified avenue for potential therapeutic improvements.

The f_1 values were 83 for CIN from the dual drug-loaded MW-NS and 26 for DOM. The acceptable limit for f_1 is less than 15, indicating significant differences between release profiles. On the other hand, the f_2 values were 34 for CIN and 42 for DOM, which did not comply with the prescribed limit of f_2, which is 50–100 [53]. The calculated f_1 and f_2 values for nanosponges synthesized via the microwave method deviated significantly from the prescribed range, signifying substantial distinctions between the release profiles of the unaltered drug and the encapsulated nanosponges. This observation indicates a pronounced escalation in the quantity of released drugs from the nanosponges, a phenomenon observed for both CIN and DOM. Intriguingly,

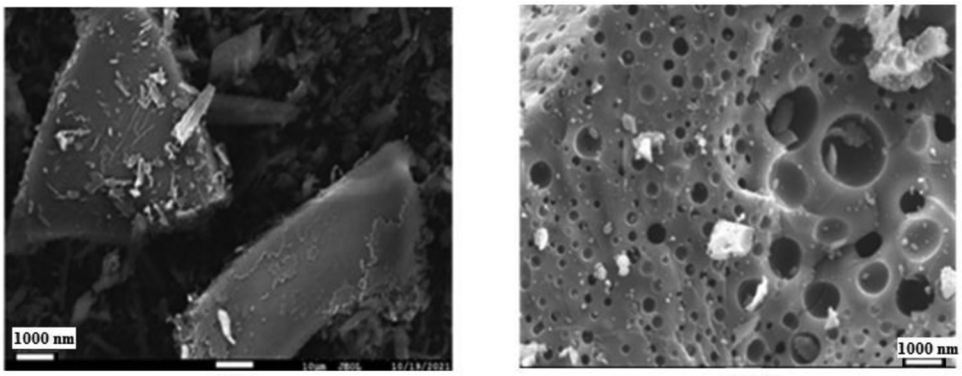

(a) (b)

Figure 6: SEM images of (a) βCD and (b) dual drug-loaded MW-NS.

the dissimilarity in release profiles was notably more pronounced in the case of CIN compared to DOM within the dual-loaded nanosponges prepared through the microwave-based method.

The R^2 for CIN and DOM from dual drug-loaded MW-NS, modeled under various kinetic release profiles, exhibited distinct trends as shown in Table 1 [54]. The amount of medication left to be released from either nanosponge affects the release of CIN, according to the release kinetics studies. This allows for a predictable and sustained release of the drug, avoiding potential adverse effects associated with high initial burst releases. By following zero-order kinetics, the drug release from nanosponges demonstrated concentration-independent behavior in the case of DOM, as shown by the greatest values of R^2. This difference in the kinetic model for the drugs could be attributed to CIN's higher aqueous solubility as compared to that of DOM [55,56], which suggests that it may readily dissolve and release from the βCD nanosponge, potentially exhibiting a first-order release profile.

3.9 Pharmacokinetic evaluation

The plasma concentration–time profiles for both drugs are shown in Figures 9 and 10. To determine the pharmacokinetic parameters, Microsoft® Excel 2019's PKSolver 2.0 add-in was utilized. The results are shown in Table 2.

Finally, dual drug-loaded MW-NS demonstrated CIN and DOM-regulated release patterns, which resulted in their absorption *in vivo*. There was a noticeable and significant difference in the bioavailability of the ordinary medicines and the nanosponges. When a commercial formulation or a simple drug suspension was administered, the absorption phase began quickly and abruptly, but when the dual drug-loaded MW-NS was administered, the absorption took longer to complete. The clearance of previously absorbed drugs and the delayed release of drugs from the nanosponges *in vivo* were responsible for the post-absorption phase that followed C_{max}. The standard formulation exhibited swift absorption kinetics for both CIN and DOM, with mean t_{max} values of 2.0 and 3.0 h,

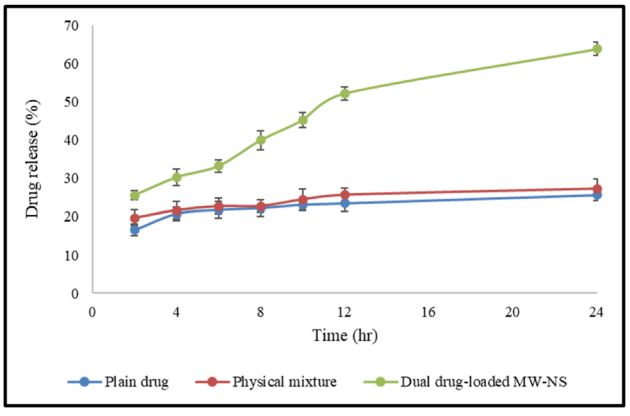

Figure 7: *In vitro* release profile of CIN from drug mixture, physical mixture with βCD, and dual drug-loaded MW-NS.

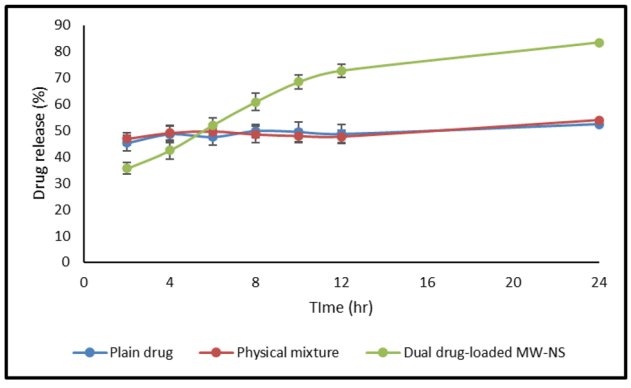

Figure 8: *In vitro* release profile of DOM from drug mixture, physical mixture with βCD, and dual drug-loaded MW-NS.

Table 1: *In vitro* drug release kinetics – model fitting

Drug	Zero order (R^2)	First order (R^2)	Higuchi square root (R^2)	Korsmeyer-Peppas (R^2)
CIN	0.8934	0.9612	0.8238	0.8451
DOM	0.9900	0.9715	0.9877	0.9781

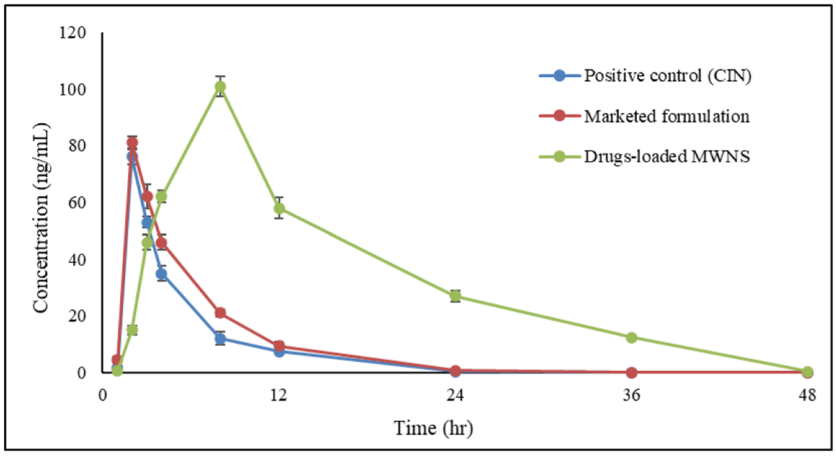

Figure 9: Comparative plasma concentration–time profile curves for CIN.

respectively. On the other hand, the mean t_{max} for CIN and DOM in the dual drug-loaded MW-NS was 4.0 and 8.0 h, respectively. The controlled-release tablet facilitated sustained plasma concentrations *in vivo*, delaying peak plasma concentrations, as seen by the significantly longer MRT for both medicines. The reference formulation at the same dose (81 ± 2.47 ng·mL^{-1}) was not as effective as the dual drug-loaded MW-NS, with a C_{max} of CIN of 101 ± 2.55 ng·mL^{-1}. As a result, in the first stage, the controlled release formulation successfully reduced drug release and subsequent absorption. The immediate release reference tablet and the controlled release dual drug-loaded MW-NS had mean $t_{1/2}$ of 3.32 ± 0.43 and 6.58 ± 0.45 h for CIN, respectively, and 5.95 ± 0.35 and 5.38 ± 0.50 h for DOM. The agreement in these values between the conventionally marketed tablet and the prolonged release MW-NS suggests that the elimination function, independent of dose form, predominantly influences the decreasing phase of the plasma concentration–time curve. Compared to CIN from the oral reference tablet, which had an $AUC_{0-\infty}$ of 430.59 ± 51.9 ng·h·mL^{-1}, the controlled release of CIN from dual drug-loaded MW-NS had an $AUC_{0-\infty}$ of 1,507.95 ±

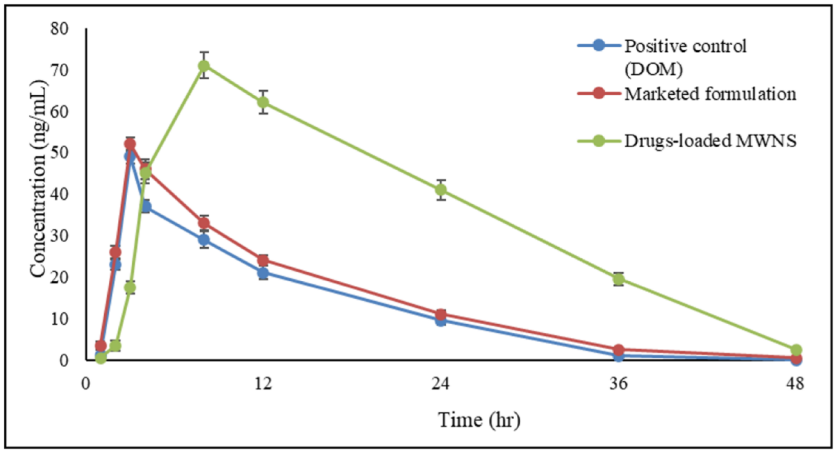

Figure 10: Comparative plasma concentration–time profile curves for DOM.

Table 2: Findings of pharmacokinetics evaluation of CIN and DOM

PK parameter	Positive control	Marketed formulation	Dual drug-loaded MW-NS
CIN			
$t_{1/2}$ (h)	3.32 ± 0.36	3.32 ± 0.43	6.58 ± 0.45$^{*,\#}$
t_{max} (h)	2 ± 0	2 ± 0	4 ± 0
C_{max} (ng·mL^{-1})	76 ± 3.18	81 ± 2.47	101 ± 2.55$^{*,\#}$
$AUC_{0\ to\ \infty}$ (ng·h·mL^{-1})	331.79 ± 49.67	430.59 ± 51.9	1507.95 ± 121.63$^{*,\#}$
MRT (h)	5.75 ± 0.54	6.05 ± 0.37	14.80 ± 0.89$^{*,\#}$
V_d (L)	7.41 ± 0.05	5.69 ± 0.07*	3.22 ± 0.06$^{*,\#}$
Cl (ng·h·L^{-1})	1.54 ± 0.02	1.19 ± 0.04*	0.34 ± 0.02$^{*,\#}$
DOM			
$t_{1/2}$ (h)	6.44 ± 0.38	5.38 ± 0.50	5.95 ± 0.35*
t_{max} (h)	3 ± 0	3 ± 0	8 ± 0
C_{max} (ng·mL^{-1})	49 ± 2.87	52 ± 3.75	71 ± 2.67$^{*,\#}$
$AUC_{0\ to\ \infty}$(ng·h·mL^{-1})	578.99 ± 39.48	689.38 ± 45.75	1676.45 ± 109.56$^{*,\#}$
MRT (h)	11.88 ± 0.88	12.53 ± 0.73	18.43 ± 0.59$^{*,\#}$
V_d (L)	6.17 ± 0.12	4.33 ± 0.08*	1.97 ± 0.04*
Cl (ng·h·L^{-1})	0.66 ± 0.02	0.56 ± 0.01*	0.23 ± 0.02$^{*,\#}$

*Significant ($p < 0.001$) compared to the pure drug (positive control).
$^{\#}$Significant ($p < 0.001$) compared to the commercial product.

121.63 ng·h·mL^{-1}. Comparably, the oral reference tablet produced 689.38 ± 45.75 ng·h·mL^{-1}, whereas the controlled release of DOM from the MW-NS had an $AUC_{0-\infty}$ of 1,676.45 ± 109.56 ng·h·mL^{-1}. As a result, the overall absorption of CIN from MW-NS was 4.54 times higher than that of its reference tablet, whereas the absorption of DOM was 2.90 times higher. This highlights the nanosponge formulation's better bioavailability, which is attributed to its enhanced dissolving and sustained release properties. In summary, the pharmacokinetic evaluation suggests that the dual drug-loaded MW-NS significantly influence the absorption, distribution, and elimination of both CIN and DOM, exhibiting notable improvements in key parameters such as $t_{1/2}$, C_{max}, AUC, MRT, V_d, and Cl compared to the positive control and the marketed formulation. The possible reasons for the improvements in these parameters were nanometer size range, improved solubility, enhanced dissolution, and improvement in overall bioavailability of CIN and DOM in nanosponge formulation compared to the positive control and marketed formulation. These findings underscore the potential of MW-NS as a viable formulation strategy to modulate drug pharmacokinetics for enhanced therapeutic outcomes.

3.10 Pharmacodynamics study

A study conducted by Mitchell et al. elucidated that inducers of gastrointestinal distress in rats, such as toxic substances or motion, prompt the consumption of non-nutritive substances like kaolin (China clay), suggesting a correlation between pica behaviors in rats and vomiting in other species [57]. Various researchers have used this as a basis for their study to evaluate the effect on the vomiting behavior in rats [33,58,59]. Consistent with this knowledge, the effects of the dual drug-loaded MW-NS on the pica reflex were examined in a rat animal model, demonstrating a clear correlation with emesis in people. The review took into account notable elements linked to human pica, such as the release of 5-HT from enterochromaffin cells, elevated c-fos expression in the nucleus tractus solitarius, and delayed gastric emptying. The results of this study are tabulated in Table 3. The findings suggest that the dual drug-loaded MW-NS effectively mitigated the duration compared to both controls during the specified time periods. Importantly, the reduced consumption of kaolin in animals upon loading the drugs into nanosponges indicates diminished gastrointestinal distress/pica. The possible reasons for the reduced consumption of kaolin in animals treated with nanosponges could be due to the enhanced solubility, drug release, and overall bioavailability of CIN and DOM in nanosponges compared to the positive control, negative control, and marketed formulation. Furthermore, the statistically significant differences observed between the drugs-loaded MW-NS and the marketed formulation align with observations from pharmacokinetic studies, substantiating the potential of nanosponge formulations in modulating both behavioral and pharmacokinetic responses.

4 Conclusion

In conclusion, this study presents a comprehensive investigation into the development and application of microwave-

Table 3: Consumption of kaolin (g) by rats of five distinct groups

Duration	Positive control	Negative control	Marketed formulation	Dual drug-loaded MW-NS
24 h	12.164 ± 1.478	17.391 ± 1.563	10.573 ± 1.496	3.440 ± 1.521*
48 h	13.452 ± 1.632	19.987 ± 1.732	12.115 ± 1.648	5.480 ± 1.746*

*Significant difference ($p < 0.001$) when compared with positive control as well as the marketed formulation.

synthesized dual-loaded CDNS for the enhanced solubility and bioavailability of CIN and DOM. The utilization of CDNS, particularly in a dual-drug loading scenario, offers a promising strategy for improving therapeutic outcomes. The microwave synthesis approach demonstrated in this research provides an environmentally friendly and efficient method for fabricating CDNS, overcoming challenges associated with traditional methods such as fusion and solvent evaporation. Physicochemical characterization confirmed the successful synthesis of dual drug-loaded nanosponges with desirable attributes, including nano-sized particles, moderately dispersed nature, and high entrapment efficiency. FTIR, DSC, and XRPD analyses supported the encapsulation of CIN and DOM within the nanosponges and their subsequent amorphization. Notably, *in vitro* drug release studies revealed a statistically significant enhancement in drug release profiles for both CIN and DOM when loaded into nanosponges compared to plain drug formulations. The controlled and sustained release profiles of the dual drug-loaded nanosponges, especially those synthesized via microwave methods, demonstrated their potential for prolonged therapeutic effects. Pharmacokinetic studies in Wistar rats further substantiated the superiority of the nanosponge formulation, exhibiting significantly improved bioavailability for both CIN and DOM compared to conventional formulations. The delayed absorption, prolonged mean residence time, and enhanced area under the plasma–time curve underscored the sustained release and dissolution-enhanced characteristics of the dual drug-loaded nanosponges. Moreover, the pharmacodynamic study using a rat emesis model provided additional evidence of the nanosponges' efficacy in mitigating gastrointestinal distress, as indicated by the reduced consumption of kaolin pellets. The observed correlations between behavioral responses and pharmacokinetic parameters further emphasize the potential therapeutic benefits of the developed nanosponge formulation. Overall, this study demonstrates the adaptability of microwave-synthesized dual drug-loaded CDNS as a promising formulation strategy, offering improved solubility, controlled release, and enhanced bioavailability for co-administered drugs. The findings suggest a potential application of these nanosponges in addressing challenges associated with combination drug therapy, especially in conditions requiring synergistic effects and improved patient compliance. However, more clinical and toxicity studies are required to explore the commercial potential of developed dual drug-loaded CDNS.

Acknowledgments: The authors are thankful to the Researchers Supporting Project number (RSPD2024R1040), King Saud University, Riyadh, Saudi Arabia, for supporting this work.

Funding information: This work was funded by the Researchers Supporting Project number (RSPD2024R1040), King Saud University, Riyadh, Saudi Arabia.

Author contributions: MV: conceptualization, methodology, investigation, software, data curation writing original draft; ND: methodology, formal analysis, data curation, software; LK: formal analysis, data curation, validation; NC: investigation, validation, software; PK: data curation, formal analysis, software; PW: conceptualization, supervision, project administration, validation; SUDW: data curation, validation, software; FS: software; data curation, formal analysis, funding acquisition, validation, resources; MA: formal analysis, data curation, validation. Finally, all the authors have read, edited, and approved the final version of the manuscript.

Conflict of interest: The authors state no conflict of interest.

Data availability statement: All data generated or analyzed during this study are included in this published article.

References

[1] Sun W, Sanderson P, Zheng W. Drug combination therapy increases successful drug repositioning. Drug Discov Today. 2016;21:1189–95.

[2] Güvenç Paltun B, Kaski S, Mamitsuka H. Machine learning approaches for drug combination therapies. Brief Bioinform. 2021;22:bbab293.

[3] Shi S, Chen H, Lin X, Tang X. Pharmacokinetics, tissue distribution and safety of cinnarizine delivered in lipid emulsion. Int J Pharm. 2010;383:264–70.

[4] Lucertini M, Mirante N, Casagrande M, Trivelloni P, Lugli V. The effect of cinnarizine and cocculus indicus on simulator sickness. Physiol Behav. 2007;91:180–90.

[5] Shazly GA, Alshehri S, Ibrahim MA, Tawfeek HM, Razik JA, Hassan YA, et al. Development of domperidone solid lipid nanoparticles: In vitro and in vivo characterization. AAPS PharmSciTech. 2018;19:1712–9.

[6] Champion MC, Hartnett M, Yen M. Domperidone, a new dopamine antagonist. Can Med Assoc J. 1986;135:457–61.

[7] Oosterveld WJ. The combined effect of cinnarizine and domperidone on vestibular susceptibility. Aviat Space Env Med. 1987;58:218–23.

[8] Amidon GL, Lennernas H, Shah VP, Crison JR. A theoretical basis for a biopharmaceutic drug classification-the correlation of in-vitro drug product dissolution and in-vivo bioavailability. Pharm Res. 1995;12:413–20.

[9] Shakeel F, Kazi M, Alanazi FK, Alam P. Solubility of cinnarizine in (Transcutol + water) mixtures: Determination, Hansen solubility parameters, correlation, and thermodynamics. Molecules. 2021;26:E7052.

[10] Mishra B, Patel BB, Tiwari S. Colloidal nanocarriers: A review on formulation technology, types and applications toward targeted drug delivery. Nanomedicine. 2010;6:9–24.
[11] Mura P. Advantages of the combined use of cyclodextrins and nanocarriers in drug delivery: A review. Int J Pharm. 2020;579:E119181.
[12] Ud Din F, Aman W, Ullah I, Qureshi OS, Mustapha O, Shafique S, et al. Effective use of nanocarriers as drug delivery systems for the treatment of selected tumors. Int J Nanomed. 2017;12:7291–309.
[13] Patra JK, Das G, Fernandes LF, Campos EVR, Rodriguez-Torres MP, Acosta-Torres LS, et al. Nano based drug delivery systems: Recent developments and future prospects. J Nanobiotechnol. 2018;16:E71.
[14] Saeedi M, Eslamifar M, Khezri K, Dizaj SM. Applications of nanotechnology in drug delivery to the central nervous system. Biomed Pharmacother. 2019;111:666–75.
[15] Kim DH, Lee SE, Pyo YC, Tran P, Park JS. Solubility enhancement and application of cyclodextrins in local drug delivery. J Pharm Investig. 2020;50:17–27.
[16] Utzeri G, Matias PMC, Murtinho D, Valente AJM. Cyclodextrin-based nanosponges: Overview and opportunities. Front Chem. 2022;10:E859406.
[17] Liu X, Li W, Xuan G. Preparation and characterization of β-cyclodextrin nanosponges and study on enhancing the solubility of insoluble nicosulfuron. IOP Conf Ser Mater Sci Eng. 2020;774:E012108.
[18] Abou Taleb S, Moatasim Y, GabAllah M, Asfour MH. Quercitrin loaded cyclodextrin based nanosponge as a promising approach for management of lung cancer and COVID-19. J Drug Deliv Sci Technol. 2022;77:E103921.
[19] Dhakar NK, Caldera F, Bessone F, Cecone C, Pedrazzo AR, Cavalli R, et al. Evaluation of solubility enhancement, antioxidant activity, and cytotoxicity studies of kynurenic acid loaded cyclodextrin nanosponge. Carbohydr Polym. 2019;224:E115168.
[20] Aboushanab AR, El-Moslemany RM, El-Kamel AH, Mehanna RA, Bakr BA, Ashour AA. Targeted fisetin-encapsulated β-cyclodextrin nanosponges for breast cancer. Pharmaceutics. 2023;15:E1480.
[21] Kumar S, Dalal P, Rao R. Cyclodextrin nanosponges: A promising approach for modulating drug delivery. In Colloid science in pharmaceutical nanotechnology. London, UK: IntechOpen; 2019.
[22] Sherje AP, Dravyakar BR, Kadam D, Jadhav M. Cyclodextrin-based nanosponges: A critical review. Carbohydr Polym. 2017;173:37–49.
[23] Singireddy A, Rani Pedireddi S, Nimmagadda S, Subramanian S. Beneficial effects of microwave assisted heating versus conventional heating in synthesis of cyclodextrin based nanosponges. Mater Today Proc. 2016;3:3951–9.
[24] Sarabia-Vallejo Á, Caja MDM, Olives AI, Martín MA, Menéndez JC. Cyclodextrin inclusion complexes for improved drug bioavailability and activity: Synthetic and analytical aspects. Pharmaceutics. 2023;15:E2345.
[25] Vij M, Dand N, Kumar L, Wadhwa P, Wani SUD, Mahdi WA, et al. Optimization of a greener-approach for the synthesis of cyclodextrin-based nanosponges for the solubility enhancement of domperidone, a BCS class II drug. Pharmaceuticals. 2023;16:E567.
[26] Vij M, Dand N, Kumar L, Ankalgi A, Wadhwa P, Alshehri S, et al. RP-HPLC-based bioanalytical approach for simultaneous quantitation of cinnarizine and domperidone in rat plasma. Separations. 2023;10:E159.
[27] Anandam S, Selvamuthukumar S. Optimization of microwave-assisted synthesis of cyclodextrin nanosponges using response surface methodology. J Porous Mater. 2014;21:1015–23.
[28] Dinde M, Galgatte U, Shaikh F. Development and evaluation of cinnarizine loaded nanosponges: Pharmacodynamic and pharmacokinetic study on Wistar rats. Int J Pharm Sci Rev Res. 2020;65:96–105.
[29] Omar SM, Ibrahim F, Ismail A. Formulation and evaluation of cyclodextrin-based nanosponges of griseofulvin as pediatric oral liquid dosage form for enhancing bioavailability and masking bitter taste. Saudi Pharm J. 2020;28:349–61.
[30] Castañeda-Hernández G, Vargas-Alvarado Y, Aguirre F, Flores-Murrieta FJ. Pharmacokinetics of cinnarizine after single and multiple dosing in healthy volunteers. Arzneimittelforschung. 1993;43:539–42.
[31] Helmy SA, El Bedaiwy HM. Pharmacokinetics and comparative bioavailability of domperidone suspension and tablet formulations in healthy adult subjects. Clin Pharmacol Drug Dev. 2013;3:126–31.
[32] Yamamoto K, Matsunaga S, Matsui M, Takeda N, Yamatodani A. Pica in mice as a new model for the study of emesis. Methods Find Exp Clin Pharmacol. 2002;24:135–8.
[33] Nakajima S. Pica caused by emetic drugs in laboratory rats with kaolin, gypsum, and lime as test substances. Physiol Behav. 2023;261:E114076.
[34] Sirisha N, Kumari S. Validated RP-HPLC method for simultaneous estimation of cinnarizine and domperidone in bulk and pharmaceutical dosage form. J Pharm Sci Innov. 2013;2:46–50.
[35] Huang M, Xiong E, Wang Y, Hu M, Yue H, Tian T, et al. Fast microwave heating-based one-step synthesis of DNA and RNA modified gold nanoparticles. Nat Commun. 2022;13:968.
[36] Hoz ADL, Alcázar J, Carrillo J, Herrero MA, Muñoz JDM, Prieto P, et al. Reproducibility and scalability of microwave-assisted reactions. In Microwave heating. London, UK: IntechOpen. 2011. doi: 10.5772/19952.
[37] Shah JJ, Mohanraj K. Comparison of conventional and microwave-assisted synthesis of benzotriazole derivatives. Indian J Pharm Sci. 2014;76:46–53.
[38] Virlley S, Shukla S, Arora S, Shukla D, Nagdiya D, Bajaj T, et al. Recent advances in microwave-assisted nanocarrier based drug delivery system: Trends and technologies. J Drug Deliv Sci Technol. 2023;87:E104842.
[39] Guineo-Alvarado J, Quilaqueo M, Hermosilla J, González S, Medina C, Rolleri A, et al. Degree of crosslinking in β-cyclodextrin-based nanosponges and their effect on piperine encapsulation. Food Chem. 2021;340:E128132.
[40] Bhattacharjee S. DLS and zeta potential–What they are and what they are not? J Controlled Rel. 2016;235:337–51.
[41] Jawaharlal S, Subramanian S, Palanivel V, Devarajan G, Veerasamy V. Cyclodextrin-based nanosponges as promising carriers for active pharmaceutical ingredient. J Biochem Mol Toxicol. 2024;38:E23597.
[42] Utzeri G, Cova TF, Murtinho D, Pais AACC, Valente AJM. Insights on macro- and microscopic interactions between confidor and cyclodextrin-based nanosponges. Chem Eng J. 2023;455:E140882.
[43] Abdelmonem R, Hamed RR, Abdelhalim SA, ElMiligi MF, El-Nabarawi MA. Formulation and characterization of cinnarizine targeted aural transfersomal gel for vertigo treatment: A pharmacokinetic study on rabbits. Int J Nanomed. 2020;15:6211–23.
[44] Zayed GM, Rasoul SAE, Ibrahim MA, Saddik MS, Alshora DH. In vitro and in vivo characterization of domperidone-loaded fast dissolving buccal films. Saudi Pharm J. 2020;28:266–73.
[45] Kumar S, Prasad M, Rao R. Topical delivery of clobetasol propionate loaded nanosponge hydrogel for effective treatment of psoriasis: Formulation, physicochemical characterization, antipsoriatic potential and biochemical estimation. Mater Sci Eng C. 2021;119:E111605.

[46] Mashaqbeh H, Obaidat R, Al-Shar'i N. Evaluation and characterization of curcumin-β-cyclodextrin and cyclodextrin-based nanosponge inclusion complexation. Polymers. 2021;13:E4073.
[47] Taleb SA, Moatasim Y, GabAllah M, Asfour MH. Quercitrin loaded cyclodextrin based nanosponge as a promising approach for management of lung cancer and COVID-19. J Drug Deliv Sci Technol. 2022;77:E103921.
[48] Khan SA, Azam W, Ashames A, Fahelelbom KM, Ullah K, Mannan A, et al. β-cyclodextrin-based (IA-Co-AMPS) semi-IPNs as smart biomaterials for oral delivery of hydrophilic drugs: Synthesis, characterization, in-vitro and in-vivo evaluation. J Drug Deliv Sci Technol. 2020;60:E101970.
[49] Pawar S, Shende P. Dual drug delivery of cyclodextrin cross-linked artemether and lumefantrine nanosponges for synergistic action using 2^3 full factorial designs. Coll Surf A. 2020;602:E125049.
[50] Caldera F, Tannous M, Cavalli R, Zanetti M, Trotta F. Evolution of cyclodextrin nanosponges. Int J Pharm. 2017;531:470–9.
[51] Singh V, Xu J, Wu L, Liu B, Guo T, Guo Z, et al. Ordered and disordered cyclodextrin nanosponges with diverse physicochemical properties. RSC Adv. 2017;7:23759–64.
[52] Salazar S, Yutronic N, Kogan MJ, Jara P. Cyclodextrin nanosponges inclusion compounds associated with gold nanoparticles for potential application in the photothermal release of melphalan and cytoxan. Int J Mol Sci. 2021;22:E6446.
[53] Kassaye L, Genete G. Evaluation and comparison of in-vitro dissolution profiles for different brands of amoxicillin capsules. Afr Health Sci. 2013;13:369–75.
[54] Askarizadeh M, Esfandiari N, Honarvar B, Sajadian SA, Azdarpour A. Kinetic modeling to explain the release of medicine from drug delivery systems. ChemBioEng Rev. 2023;10:1006–49.
[55] Abdelrahman MM. Simultaneous determination of cinnarizine and domperidone by area under curve and dual wavelength spectrophotometric methods. Spectrochim Acta A. 2013;113:291–6.
[56] Tambawala TS, Shah PJ, Shah SA. Orally disintegrating tablets of cinnarizine and domperidone: A new arsenal for the management of motion sickness. J Pharm Sci Tech Mgmt. 2015;1:81–97.
[57] Mitchell D, Laycock J, Stephens W. Motion sickness-induced pica in the rat. Am J Clin Nutr. 1977;30:147–50.
[58] Horn CC, De Jonghe BC, Matyas K, Norgren R. Chemotherapy-induced kaolin intake is increased by lesion of the lateral parabrachial nucleus of the rat. Am J Physiol Regul Integr Comp Physiol. 2009;297:R1375–82.
[59] Nakajima S. Running-based pica and taste avoidance in rats. Learn Behav. 2018;46:182–97.